A Novel Anionic Gold−Indium Cluster Compound: Synthesis and Molecular and Electronic Structure

François P. Gabbaï,[†] Sai-Cheong Chung,[‡] Annette Schier,[†] Sven Krüger,[‡] Notker Rösch,*[,‡] and Hubert Schmidbaur*[,†]

Anorganisch-chemisches Institut and Lehrstuhl für Theoretische Chemie der Technischen Universität München, Lichtenbergstrasse 4, D-85747 Garching, Germany

Received June 12, 1997[⊗]

The insertion of InBr into the Au−Br bond of [(Ph_3P)AuBr] in tetrahydrofuran (thf) in the presence of [(CH_2-PPh_2)$_2$] (dppe) leads to the formation of an orange complex [(dppe)$_2$Au]$^+$[(dppe)$_2$$Au_3In_3Br_7$(thf)]$^-$, **2**. Analytical, spectroscopic, and X-ray structural investigations showed that this product is an anionic analogue of a neutral chloride complex [(dppe)$_2$$Au_3In_3Cl_6(thf)_3$], **1**, prepared recently. Both complexes have an Au_3In_3 cluster core of approximate C_{2v} symmetry with one extremely short Au−Au bond [Au1−Au3 2.575(1) Å] as part of a quasi-linear array P1−Au1−Au3−P4, suggesting the presence of a bis(phosphine) complex of the neutral Au_2 molecule as part of the cluster. The third gold atom (Au2) is then assigned oxidation state +1. To gain deeper insight into the structure and bonding of this novel class of gold cluster compounds, regarding mainly the peculiar cluster geometry, the charge distribution, and the oxidation states, a series of scalar relativistic all-electron density functional (DF) calculations on model systems has been performed. As a model for **1**, the neutral cluster {Au_3(PH_3)$_4$[$InCl_2$-(H_2O)]$_3$} was studied. For the examination of the geometry of complexes **1** and **2**, the cluster Au_3(PH_3)$_4$$I_3$ has been considered as a further simplified model, where iodine replaces the InX_2(thf) units. Experimental and calculated cluster geometries agree satisfactorily, and the formal oxidation states of the gold atoms (0 for Au1 and Au3, +1 for Au2) could be confirmed, but for the In centers no interpretable differences of the Mulliken charges were found.

1. Introduction

The cluster chemistry of gold has been an extremely active area of research for more than two decades. The emerging rules of stoichiometry, structure, and bonding of *homoatomic* gold clusters in particular are providing a consistent and transparent taxonomy of a large variety of cluster species.[1] The field of *heteroatomic* gold clusters is far less developed,[2] and only a small number of metals have been considered as components of mixed-metal aggregates.[3] While at least a few of the late transition metals, namely, those neighboring gold in the periodic table, have been included in the more recent investigations in several laboratories,[3,4] there is a complete lack of information on discrete gold clusters containing the more electropositive transition or main group metals.[5]

A deeper knowledge of such clusters is desirable, however, for a number of reasons: (1) Mixed-metal clusters of well-defined stoichiometry and structure are important model systems for bulk alloys and their surfaces. (2) Clusters composed of metals with strongly different atomic radii and electronegativities are expected to show tunable and thus more selective reactivity in stoichiometric and catalytic reactions. (3) The theory of chemical bonding in *hetero* clusters and nanoparticles is only emerging,[6−9]and it has to date been developed mainly for binary systems with few heteroatoms which are not too different in their element characteristics from the parent gold component.[7] (4) Depending on the electronegativity of the admixed metal components, gold can be assigned not only low, nonintegral positive oxidation states but even nonintegral oxidation states approaching negative unity as in aurides of the type Cs^+Au^-. "Reversing the polarity" of gold is thus not an unreasonable concept for cluster chemistry, as it has already been demonstrated for bulk Zintl phases containing gold.[5]

Following up a program on gold clusters with interstitial *nonmetals* (B, C, N, O, Cl and their homologues),[10] a systematic study has therefore recently been initiated to probe gold cluster formation with electropositive main group metals. In the present report some results on the binary Au/In system are presented. A preliminary account has been published,[11] the contents of which regarding preparation and crystal structure is not duplicated here. The results are included in the discussion, however, since, as an important extension of the previous[11] and present experimental work, we recently also turned to theoretical studies of these important prototypes. Density functional calculations including relativistic effects have been employed for studying a number of pertinent problems and have proven extremely useful for describing structure and bonding in gold hetero clusters.[12,13]

† Anorganisch-chemisches Institut.
‡ Lehrstuhl für Theoretische Chemie.
⊗ Abstract published in *Advance ACS Abstracts,* November 1, 1997.

(1) Hall, K. P.; Mingos, D. M. P. *Prog. Inorg. Chem.* **1984**, *32*, 237.
(2) Mingos, D. M. P.; Watson, M. J. *Adv. Inorg. Chem.* **1992**, *39*, 327.
(3) (a) Teo, B. K.; Zhang, H. *Coord. Chem. Rev.* **1995**, *143*, 611. (b) Pignolet, L. H.; Aubart, M. A.; Craighead, K. L.; Gould, R. A. T.; Krogstad, D. A.; Wiley, J. S. *Coord. Chem. Rev.* **1995**, *143*, 219.
(4) (a) Steggerda, J. J. *Comments Inorg. Chem.* **1992**, *11*, 113. (b) Strähle, J. *J. Organomet. Chem.* **1995**, *488*, 15.
(5) (a) Schmidbaur, H. *Gold Bull.* **1990**, *23*, 11. (b) Mingos, D. M. P.; Powell, H. R.; Stolberg, T. L. *Transition Met. Chem.* **1992**, *17*, 334.
(6) Schmid, G. *Clusters and Colloids*; VCH: Weinheim, 1994.
(7) (a) Mingos, D. M. P.; Johnson, R. J. *Struct. Bonding* **1987**, *68*, 29. (b) Mingos, D. M. P. *J. Cluster Sci.* **1992**, *3*, 397.
(8) Mingos, D. M. P.; Wales, D. J. *Introduction to Cluster Chemistry*; Prentice-Hall: Englewood Cliffs, NJ, 1990.
(9) Heiz, U.; Vayloyan, A.; Schumacher, E.; Yeretzian, C.; Stener, M.; Gisdakis, P.; Rösch, N. *J. Chem. Phys.* **1996**, *105*, 5574.
(10) (a) Schmidbaur, H. *Chem. Soc. Rev.* **1995**, *24*, 391. (b) Blumenthal, A.; Beruda, H.; Schmidbaur, H. *J. Chem. Soc., Chem. Commun.* **1993**, 1005.
(11) Gabbai, F. P.; Schier, A.; Schmidbaur, H. *Inorg. Chem.* **1995**, *34*, 3844.

S0020-1669(97)00725-8 CCC: $14.00

The theoretical treatment of large heavy-metal clusters is a challenging task, but it has been demonstrated that calculations on suitable models of reduced complexity make the problems tractable, yet also lead to meaningful fundamental conclusions.[13,14] This strategy has also been successfully used in the present study by introducing simple pseudoligands with frontier orbital characteristics and electron counts similar to those of the ligands in the synthesized systems.

2. Experimental Section

2.1. General Procedures. All experiments were carried out under an atmosphere of dry, purified nitrogen. Glassware was dried and filled with nitrogen, and solvents were distilled and kept under nitrogen. NMR: Jeol GX 400; TMS and 85% aqueous H_3PO_4 as external standards for ^1H and ^{31}P NMR, respectively. MS: Finnigan MAT 90. Microanalyses: In-house analyzers (by combustion). InBr was prepared by melting together 2 equiv of indium powder with 1 equiv of $InBr_3$ under vacuum at 375 °C and purified through sublimation under the same conditions. Ph_3PAuBr was prepared by the reaction of NaBr with Ph_3PAuCl in the two-phase system $CHCl_3/H_2O$ and purified by recrystallization from a $CHCl_3$/hexane solution.

2.2. Preparation of $[(dppe)_2Au]^+[(dppe)_2Au_3In_3Br_7(thf)]^-$ (2). InBr (0.10 g, 0.51 mmol), Ph_3PAuBr (0.27 g, 0.5 mmol), and dppe (0.20 g, 0.5 mmol) were mixed as solids and cooled to −78 °C. Thf (5 mL) was then added to the mixture. With stirring, the reaction mixture was allowed to reach room temperature, during which time a yellowish precipitate had formed. After 3 h at 20 °C the precipitate was isolated through filtration. Addition of CH_2Cl_2 (5 mL) to the precipitate followed by filtration yielded an orange solution. A layer of hexane (5 mL) was slowly allowed to diffuse into this CH_2Cl_2 solution at −25 °C, which resulted in the precipitation of 0.10 g (24% yield based on gold) of an orange crystalline compound **2** (mp 105° C dec). Elemental anal. for $C_{108}H_{104}Au_4Br_7In_3OP_8$. Calcd: C, 38.6; H, 3.1. Found: C, 38.0; H, 3.4. ^{31}P NMR {^1H} (109.3 MHz) δ (ppm): 18.0 (4P, $[(dppe)_2Au]^+$), 31.3 (2P), 56.3 (2P, $[(dppe)_2Au_3In_3Br_7(thf)]^-$). ^1H NMR (399.8 MHz) δ (ppm): 1.76, 3.54 (br, 8H, thf); 2.43 (br, 8H, C*H*$_2$-$[(dppe)_2Au]^+$), 3.10 (4H), 3.42 (4H, br, C*H*$_2$-$[(dppe)_2Au_3In_3Br_7$-(thf)]$^-$), 6.96−7.67 and 8.05 (m, 80H, Ph-C*H*). MS (FAB): *m*/*z* 993 ($[(dppe)_2Au]^+$, 100).

2.3. X-ray Crystallography. A specimen of suitable quality and size (0.1 × 0.25 × 0.40 mm) was mounted in a glass capillary and used for measurements of precise cell constants and intensity data collection. Diffraction measurements were made on an Enraf-Nonius CAD-4 diffractometer using graphite-monochromated Mo Kα radiation (λ = 0.710 73 Å) with the ω scan mode at −68 °C. An Lp correction was applied, and intensity data were corrected for decay (−14.1%) and absorption effects (ψ-scans, T_{min}/T_{max} = 0.449/0.999). The structure was solved by direct methods (SHELXTL-PLUS) and completed by full-matrix least-squares techniques (SHELXL-93).

$C_{108}H_{104}Au_4Br_7In_3OP_8$: M = 3357.37, monoclinic, a = 12.681(1) Å, b = 20.139(1) Å, c = 44.182(4) Å, β = 91.06(1)°, space group $P2_1/c$ (No. 14), Z = 4, D_c = 1.977 g cm^{-3}, $F(000)$ = 6352 e, μ(Mo Kα) = 84.2 cm^{-1}; 16 424 intensity data were measured up to (sin $\theta/\lambda)_{max}$ = 0.59 Å^{-1}, of which 16 349 independent structure factors were used for refinement. All non-H atoms were refined with anisotropic displacement parameters. All H atoms were placed in idealized calculated positions and allowed to ride on their carbon atoms with fixed isotropic contributions [$U_{(iso)fix} = 1.5U_{eq}$(C) for all methylene and 0.08 for all phenyl H atoms]. The function minimized was $\{[\Sigma w(F_o^2 - F_c^2)^2]/\Sigma[w(F_o^2)^2]\}^{1/2}$, with $w = 1/\sigma^2(F_o^2)+(ap)^2 + (bp)$, $p = (F_o^2 + 2F_c^2)/3$, and a = 0.0855, b = 241.16. The final R_w and R_1 [based on $\Sigma(||F_o| - |F_c||)/\Sigma|F_o|$] were 0.1621 and 0.0665, respectively, for 988 refined parameters.

2.4. Computational Details. Calculations were performed in an all-electron fashion by means of the scalar relativistic linear combination of Gaussian-type orbitals density functional (LCGTO-DF) method.[15,16] The local spin density approximation (LSDA) for the exchange-correlation functional[17] was applied during the self-consistency cycles. This model functional often overestimates ligand binding energies, yet it is known to yield accurate geometry and vibrational data.[18] We refrained from using a more accurate, yet computationally more demanding gradient-corrected functional since in the discussion of energetic aspects we are mainly interested in a comparison of trends.

The Gaussian-type molecular orbital basis sets for the atoms Au, P, O, and H were taken as in previous investigations on other gold compounds.[19,20] Listing the number of exponents of the uncontracted bases in parentheses and the size of the contracted ones in brackets, the basis sets used are as follows: Au(21s,17p,11d,7f) → [11s,10p,-7d,3f], P(12s,9p,1d) → [5s,4p,1d], O(9s,5p,1d) → [4s,3p,1d], and H(6s,1p) → [4s,1p]. Basis sets of comparable quality were chosen for In, I, and Cl: In(18s,14p,8d) → [7s,5p,4d],[21,22] I(17s,14p,8d) → [7s,5p,4d],[22] and Cl(12s,9p,1d) → [5s,4p,1d].[23,24] These atomic basis sets were contracted in a generalized fashion using atomic LDA eigenvectors. The charge density and the exchange-correlation potential were represented by auxiliary Gaussian-type basis sets.[15] The corresponding s- and $d(r^2)$-type functions were generated in a standard fashion.[15] For the heavier atoms, Au, In, I, and Cl, only every second $d(r^2)$-type function was used. In addition, a set of three p-type and three d-type polarization exponents was employed for each atomic center, except for O and H, where only p-type polarization functions were taken into account. The p-exponents were 0.1, 0.4375, and 1.562; the d-exponents are scaled by a factor of 2. The auxiliary basis sets were left uncontracted.

3. Preparation and Properties of a Novel Anionic Gold/Indium Cluster Complex

Preliminary work has shown that insertion of indium(I) halides [InX] into the Au−X bonds of gold(I) halide complexes [LAuX] can give ready access to mixed-metal mixed-valent Au/In cluster species.[11] Thus treatment of [InCl] with $[Ph_3PAuCl]$ in the presence of $[Ph_2PCH_2CH_2PPh_2]$ (dppe) in tetrahydrofuran (thf) affords the cluster $[(dppe)_2Au_3In_3Cl_6(thf)_3]$, **1** (eq 1). In

$$3[(Ph_3P)AuCl] + 3[InCl] + 2[dppe] + 3[thf] \rightarrow 3[Ph_3P] + \underset{\mathbf{1}}{[(dppe)_2Au_3In_3Cl_6(thf)_3]} \quad (1)$$

attempts to prepare the analogous bromide compound, we now reacted [InBr] with $[Ph_3PAuBr]$ and [dppe] in approximately equimolar quantities in thf at −78 °C. A yellow precipitate formed, which could be crystallized from dichloromethane/hexane at −25 °C (24% yield of orange crystals, mp 105 °C dec). Solutions in CD_2Cl_2 show three resonances of the relative intensities 4:2:2 in the $^{31}P\{^1H\}$ NMR spectrum (δ = 18.0, 31.3, and 56.3 ppm). In the ^1H NMR spectra there are the multiplet signals for metal-coordinated [thf] at δ = 1.76 and 3.54 ppm and broad resonances for three types of CH_2 groups at δ = 2.43 (8H), 3.10 (4H), and 3.42 ppm (4H), complemented by an extended multiplet of aryl resonances δ = 6.96−8.05 ppm (m, 80H). In FAB mass spectra the prominent peak for *m*/*z* = 993

(12) Görling, A.; Rösch, N.; Ellis, D. E.; Schmidbaur, H. *Inorg. Chem.* **1991**, *30*, 3986.
(13) Häberlen, O. D.; Schmidbaur, H.; Rösch, N. *J. Am. Chem. Soc.* **1994**, *116*, 8241.
(14) Rösch, N.; Görling, A.; Ellis, D. E.; Schmidbaur, H. *Angew. Chem., Int. Ed. Engl.* **1989**, *28*, 1357.
(15) Dunlap, B. I.; Rösch, N. *Adv. Quantum Chem.* **1990**, *21*, 317.
(16) Rösch, N.; Krüger, S.; Mayer, M.; Nasluzov, V. A. In *Recent Developments and Applications of Modern Density Functional Theory*; Seminario, J. M., Ed.; Elsevier: Amsterdam, 1996; p 497.
(17) Vosko, S. H.; Wilk, L.; Nusair, M. *Can. J. Phys.* **1980**, *58*, 1200.
(18) Ziegler, T. *Chem. Rev.* **1991**, *91*, 651.
(19) Häberlen, O. D.; Rösch, N. *J. Phys. Chem.* **1993**, *97*, 4970.
(20) Chung, S.-C.; Krüger, S.; Schmidbaur, H.; Rösch, N. *Inorg. Chem.* **1996**, *35*, 5387.
(21) Huzinaga, S. *J. Chem. Phys.* **1979**, *71*, 1980.
(22) Poirier, R.; Kari, R.; Cszimadia, I. G. *Handbook of Gaussian Basis Sets*; Elsevier: New York, 1985.
(23) Veillard, A. *Theor. Chim. Acta* **1968**, *12*, 405.
(24) Huzinaga, S. *Gaussian Basis Sets for Molecular Calculations*; Elsevier: New York, 1984.

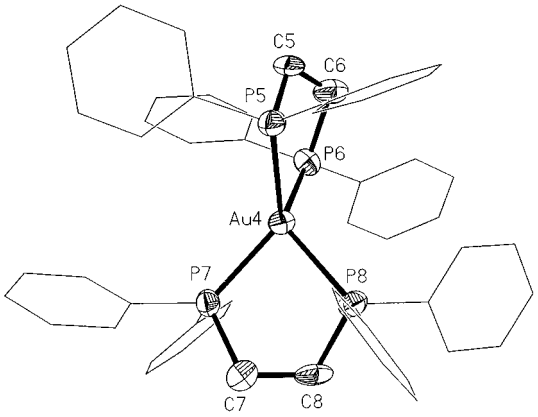

Figure 1. Molecular structure of $[(dppe)_2Au]^+$ with atomic numbering (hydrogen atoms omitted for clarity). Selected bond lengths (Å) and angles (deg): Au4−P5 2.391(5), Au4−P6 2.410(6), Au4−P7 2.399(5), Au4−P8 2.403(5); P5−Au4−P6 85.4(2), P5−Au4−P7 129.5(2), P5−Au4−P8 122.6(2), P6−Au4−P7 118.7(2), P6−Au4−P8 118.7(2), P7−Au4−P8 85.9(2).

suggests the presence of $[(dppe)_2Au]^+$ as the cationic component, which agrees well with the ^{31}P and ^1H resonances in the NMR spectra at $\delta = 18.0$ and 2.43 ppm, respectively. The limited elemental analysis data are in agreement with the complex formula $[C_{108}H_{104}Au_4Br_7In_3OP_8]$ finally set up after the solution of the X-ray crystal structure (below). This formula can be reduced to the ionic components $[(dppe)_2Au]^+[(dppe)_2Au_3In_3Br_7(thf)]^-$, which accounts for the analytical and spectroscopic data. Equation 2 is tentatively proposed for the formation of the unexpected product. The stoichiometry of the

$$4[(Ph_3P)AuBr] + 3[InBr] + 4[dppe] + [thf] \rightarrow 4[Ph_3P] + \underset{\mathbf{2}}{[(dppe)_2Au]^+[(dppe)_2Au_3In_3Br_7(thf)]^-} \quad (2)$$

anion of compound **2** is related to the composition of the neutral chloride analogue (**1**, above) in that it features an additional bromide anion replacing two thf donor molecules. This introduction of an anion at the cluster then requires the presence of a cation in the form of $[(dppe)_2Au]^+$.

4. Crystal and Molecular Structure of the Cluster Compound

Compound **2** crystallizes (from dichloromethane/hexane at −25 °C) as orange monoclinic needles (space group $P2_1/c$, $Z = 4$). The crystal lattice is composed of independent $[(dppe)_2Au]^+$ cations and $[(dppe)_2Au_3In_3Br_7(thf)]^-$ cluster anions with no unusually close interionic contacts. There are no solvent molecules present in the interstices between the two sorts of ionic components. Neither of the ions has a crystallographically imposed element of symmetry, but the core of the cation approaches quite closely the symmetry of point group S_4 (Figure 1), while the core of the anion obeys mirror symmetry very closely [the mirror plane being defined by Au2, In1, In2, Br7, O1, and In3 (Figure 2)].

There is precedent for the structure of the $[(dppe)_2Au]^+$ *cation*, which has been determined also as a component of other salts at least three times.[14,25,26] A brief comparison of essential differences of structural details shows that the conformation of the two five-membered rings (with the gold atom as a spiro center) is rather flexible and adjusts very easily to a changing crystal environment.

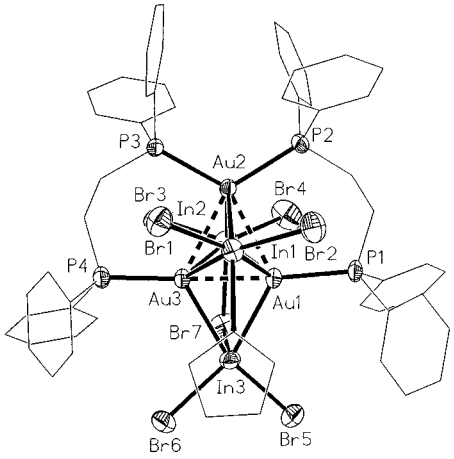

Figure 2. Molecular structure of $[(dppe)_2Au_3In_3Br_7(thf)]^-$ with atomic numbering (hydrogen atoms omitted for clarity). Selected bond lengths (Å) and angles (deg): Au1−Au2 2.860(1), Au1−Au3 2.575(1), Au2−Au3 2.858(1), Au1−In1 2.828(2), Au1−In2 2.950(2), Au1−In3 2.761(2), Au1−P1 2.300(5), Au2−In1 2.973(1), Au2−In2 2.889(2), Au2−P2 2.377(5), Au2−P3 2.381(5), Au3−In1 2.932(2), Au3−In2 2.922(2), Au3−In3 2.826(2), Au3−P4 2.288(5), In1−Br1 2.594(3), In1−Br2 2.579(3), In1−O1 2.297(13), In2−Br3 2.579(3), In2−Br4 2.582(3), In2−Br7 2.763(3), In3−Br5 2.613(3), In3−Br6 2.606(3), In3−Br7 2.785(3); Au2−Au1−Au3 63.18(3), Au1−Au2−Au3 53.52(2), Au1−Au3−Au2 63.29(3), P1−Au1−Au3 173.47(14), P4−Au3−Au1 178.5(3), In2−Br7−In3 85.68(8).

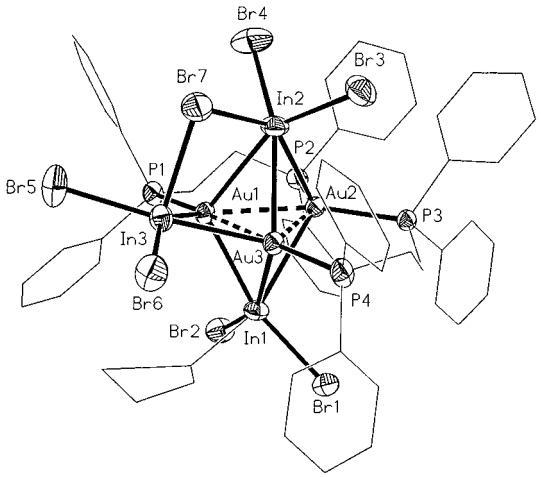

Figure 3. View of the structure of $[(dppe)_2Au_3In_3Br_7(thf)]^-$ showing the bridging of the shortest edge of the gold triangle Au1−Au3 by In3 as well as the bridging two-coordinate bromine atom Br7 between In2 and In3.

The $[Au_3In_3]$ metal core of the *anion* closely resembles that of the neutral molecule **1**. Isosceles triangles of three gold and three indium atoms are at right angles to each other, leading to an arrangement where two of the indium atoms (In1/2) are capping the gold triangle on both faces, while the third indium atom (In3) is bridging the shortest edge of the gold triangle (Au1−Au3, Figure 3). The two long edges, Au1−Au2 and Au2−Au3, are spanned by the dppe ligands.

All three indium atoms bear two terminal bromine atoms each (Br1/2, Br3/4, and Br5/6, respectively), but In1 is further coordinated to one thf molecule, while In2 and In3 are bridged by a two-coordinate bromine atom (Br7). This ligand distribution makes the two sides of the basic gold triangle different, thus contrasting with the situation in compound **1**, where the molecular cluster core obeys C_{2v} point group symmetry (Figure 4).[11] Consistent with the situation in molecule **1**, however, all

(25) Harker, C. S. W.; Tekink, R. T.; Whitehouse, M. W. *Inorg. Chim. Acta* **1991**, *181*, 23.
(26) Berners-Price, S. J.; Mazid, M. A.; Sadler, P. J. *J. Chem. Soc., Dalton Trans.* **1984**, 969.

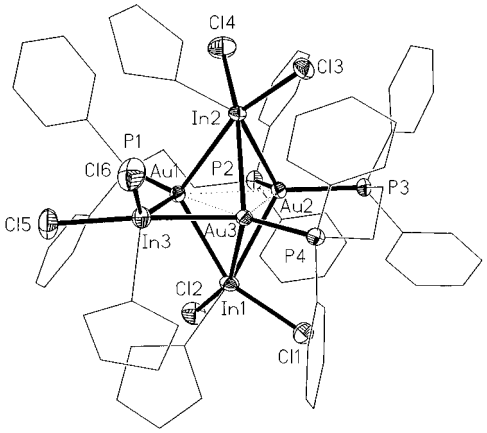

Figure 4. Molecular structure of $(dppe)_2Au_3(InCl_2thf)_3$ (hydrogen atoms omitted for clarity).[11]

three indium vertices of the cluster have three external electron pair donor ligands providing a total of six ligand electrons.

The most intriguing structural details of clusters **1** and **2** are the short distances between atoms Au1 and Au3 of only 2.562(1)/2.575(1) Å, which suggest particularly strong metal−metal interactions. These gold atoms bear only one phosphine donor ligand each, and there is conspicuous linearity of the axis P1−Au1−Au3−P4, reminiscent of the structure proposed for as yet unconfirmed phosphine complexes [L−Au−Au−L] of the dinuclear gold molecule Au_2.[5] It is therefore tempting to assign an oxidation state of 0 to the gold atoms Au1 and Au3, but +1 to Au2. The indium atoms In1 and In2 are then to be classified as +2, and In3 as +1.[11]

The gold atom Au2 bears two phosphine donor units, and its distances from Au1 and Au3 are much longer and in a standard range for many other gold clusters.

In summary, therefore, the structures of the Au_3In_3 clusters in the chloride and bromide complexes **1** and **2** are surprisingly similar, suggesting a pronounced local minimum of energy for this type of stoichiometry and organization in gold/indium cluster chemistry. It should be pointed out that there is no straightforward way of assigning an electron count or oxidation state to the four types of metal atoms (two types of gold and two types of indium atoms) using standard qualitative rules of cluster chemistry. A theoretical study of the electronic structure of this prototype seemed therefore highly desirable.

5. Theoretical Investigations

To gain deeper insight into the structure and bonding of this novel class of gold cluster compounds, a series of density functional (DF) calculations on model systems has been carried out. An accurate scalar relativistic DF approach[16,27] has been employed to account for the fact that a theoretical description of gold chemistry has to properly consider both relativistic and correlation effects.[16,28] The main objectives of our theoretical studies were a clarification of the charge distribution in the cluster compounds and support for the preliminary assignment of oxidation states to the various atoms in the Au_3In_3 metal core; furthermore, we aimed at a rationalization of the peculiar geometry of the central Au_3 unit of these Au/In clusters. Finally, we have also examined how strongly the phosphine and the $(InCl_2(thf))$ moieties are bound to the cluster core.

5.1. Model System. To examine the charge distribution of the Au/In clusters, which all exhibit a similar geometry in their central Au_3In_3 unit, the more symmetric compound $(dppe)_2Au_3(InCl_2(thf))_3$ (Figure 4) was examined as an example. The ligands had to be simplified to some extent to render the computations tractable. For this purpose, the thf groups were modeled by water ligands, which exhibit qualitatively the same frontier orbitals at the oxygen center bound to In. The dppe ligands used in the experiment were approximated by simple phosphines, PH_3. As shown in a previous study, PH_3 is a satisfactory model for larger phosphine ligands like PMe_3 or PPh_3, in particular with respect to structural aspects.[19] On the other hand, one should keep in mind that PH_3 is a weaker electron donor; thus, binding energies and charge separations will likely be underestimated.[19] (On the other hand, the LDA approximation used often tends to overestimate binding energies.) The symmetry of the resulting model cluster $Au_3(PH_3)_4(InCl_2H_2O)_3$ has been idealized to C_s, the mirror plane being defined by the three In atoms. We derived averaged bond lengths and angles from the experimental data, treating the two μ_3-In groups ($InCl_2H_2O$) as equivalent. The geometrical parameters employed for the central Au−In cluster core are as follows: d(Au1−Au3) = 2.562 Å, d(Au1/3−Au2) = 2.935 Å, d(Au1/3−In1) = 2.846 Å, d(Au2−In1) = 2.976 Å, and d(Au1/3−In3) = 2.809 Å. For the $InCl_2H_2O$ groups we used d(In1−Cl) = 2.442 Å, d(In3−Cl) = 2.453 Å, d(In1−O) = 2.311 Å, d(In3−O) = 2.336 Å, ∠(Cl−In1−Cl) = 97.95°, ∠(Cl−In3−Cl) = 96.70°, ∠(Cl−In1−O) = 89.48°, ∠(Cl−In3−O) = 86.75°, ∠(Au1/3−In1−O) = 99.03°, and ∠(Au1/3−In3−O) = 116.50°.

The parameters related to the phosphine ligands are d(Au1−P1) = 2.306 Å, d(Au2−P2) = 2.394 Å, ∠(In1−Au2−P2,3) = 107.45°, and ∠(In1−Au1/3−P1,4) = 114.85°. For the phosphine and water ligands, the following internal geometry parameters were used: d(P−H) = 1.415 Å, ∠(H−P−H) = 93.3°, d(O−H) = 0.96 Å, and ∠(H−O−H) = 104.5°.[29]

5.2. Charge Distribution. The charge distribution of the model cluster compound $Au_3(PH_3)_4(InCl_2H_2O)_3$ has been examined in a Mulliken analysis, and the results have been evaluated by comparison of Mulliken charges of various subunits of this system. Mulliken charges are known to have some serious deficiencies, in particular when interpreted in an absolute fashion. However, in a comparative study like the one carried out here, they have often proven quite useful. The following discussion will confirm this rather general experience.

In Figure 5 the effect of the In groups L = $(InCl_2H_2O)$ on the central gold triangle is shown. The L groups, which exhibit similar geometries independent of coordination, act as electron-withdrawing moieties since in the isolated group In is in the formal oxidation state +2 (Mulliken charges: In +0.61 au, Cl −0.37 au, H_2O +0.13 au). As gold is a rather electronegative metal, the charge transfer to the L groups is limited. Addition of μ_2-L or μ_3-L groups induces a charge of about 0.1 au on the gold triangle, which is not enhanced by the concerted effect of both types of ligand groups. The charge distribution in the Au_3 moiety changes due to the addition of L moieties (Figure 5): while Au1/3 are positively and Au2 is negatively charged in Au_3, the charges change signs in Au_3L_3. Although differently coordinated, the μ_2- and μ_3-L groups exhibit a very similar internal charge distribution. All In atoms carry a charge of about 0.5 au (Figure 5).

The addition of electron-donating phosphine ligands has, not unexpectedly, a considerable effect on the charge distribution in the cluster (Figure 6). Phosphine ligation reverses the sign of charge separation in the bare cluster Au_3 and enhances the donating ability of the Au_3 moiety. This leads to larger negative

(27) Häberlen, O. D.; Rösch, N. *Chem. Phys. Lett.* **1992**, *199*, 491.
(28) Pyykkö, P. *Chem. Rev.* **1988**, *88*, 563.
(29) Weast, R. C. *CRC Handbook of Chemistry and Physics*, 61st ed.; CRC Press, Boca Raton, 1980.

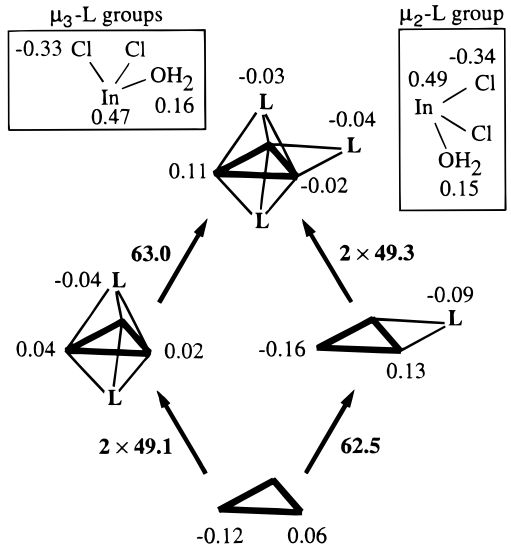

Figure 5. Mulliken population analysis of the clusters Au_3L_n, n = 0−3, L = $InCl_2H_2O$, at the experimental geometry. The Au_3 subunit is depicted as a solid triangle. Detailed charge distributions of the L groups of the cluster Au_3L_3 are given in boxes. The reaction arrows interconnecting the different species are labeled with the binding energies of the newly attached L groups in kcal/mol.

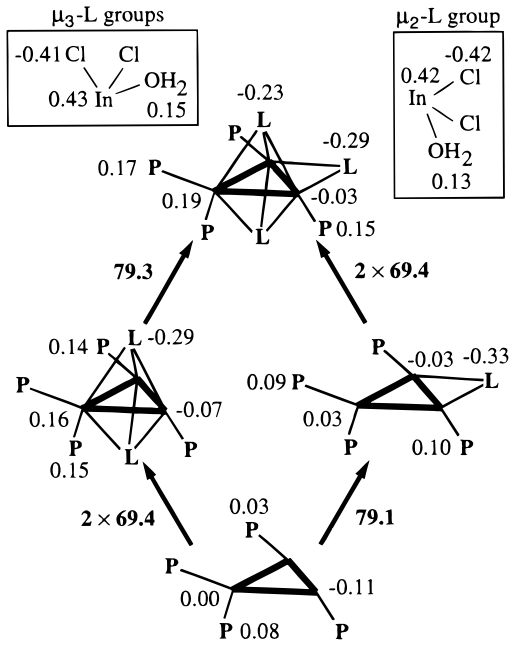

Figure 6. Mulliken population analysis of the phosphine-ligated clusters $Au_3(PH_3)_4L_n$, $n = 0-3$, L = $InCl_2H_2O$, at the experimental geometry. The Au_3 subunit is depicted as a solid triangle. The phosphine ligands are abbreviated by P. Detailed charge distributions of the L groups of the cluster Au_3L_3 are given in boxes. The reaction arrows interconnecting the different species are labeled with the binding energies of the newly attached L groups in kcal/mol.

charges of the L groups. Both types, μ_2-L and μ_3-L, exhibit a charge of about 0.3 au if they are added separately. In the complete cluster their charge is slightly smaller, −0.29 au for μ_2-L and −0.23 au for μ_3-L (Figure 6). The increased oxidation of the gold triangle as a consequence of L group addition is nicely reflected by the Mulliken charges of about −0.2 au for $Au_3(PH_3)_4$, 0.0 au for $Au_3(PH_3)_4(\mu_2\text{-L})$ and $Au_3(PH_3)_4(\mu_3\text{-L})_2$, and 0.1 au in the full model cluster. A comparison of the population data for clusters with and without phosphine ligands shows that the electronic charge donated by the phosphines (−0.64 au) is mainly taken up by the Cl atoms in the In groups (−0.48 au), to a smaller extent only by the In atoms (−0.15 au). The Mulliken charges of +0.19 au for Au2 and −0.03 au for Au1/3 in $Au_4(PH_3)_4L_3$ provide further support for the earlier assignment of oxidation states +1 and 0,[11] respectively, which was based on geometry arguments as well as on Mössbauer spectroscopy investigations. Surprisingly, no significant differences were found between the Mulliken charges of the two types of In ligand moieties. Thus, on the basis of the present results, we prefer to assign an intermediate formal oxidation state between +1 and +2 to both of these In units. We are unable to confirm the tentative interpretation[11] of μ_2-In as In(+1) and μ_3-In as In(+2) suggested by the different coordination of these two groups.

Table 1. Binding Energies D_e (in kcal/mol) of Phosphine Ligands[a] in $Au_3(PH_3)_4L_n$, $n = 0-3$, L = $(InCl_2H_2O)$

system	P1/4H3	P2/3H3	av[b]
$Au_3(PH_3)_4$	41.5	30.7	28.6
$Au_3(PH_3)_4L$	48.0	21.4	32.7
$Au_3(PH_3)_4L_2$	51.4	29.5	38.7
$Au_3(PH_3)_4L_3$	56.5	32.3	42.9

[a] For the definition of P1/4H3 and P2/3H3 see Figure 4. [b] Average binding energy determined from the reaction $Au_3(PH_3)_4L_n \rightarrow Au_3L_n + 4PH_3$.

Table 2. Average Binding Energies[a] D_e (in kcal/mol) of Phosphine Ligands in $Au_3(PH_3)_4L_n^{m+}$, $n = 0-2$, $m = 0-2$, L = $(InCl_2H_2O)$

system	$m = 0$	$m = 1$	$m = 2$
$Au_3(PH_3)_4$	28.6	47.0	69.4
$Au_3(PH_3)_4L$	32.7	45.4	62.3
$Au_3(PH_3)_4L_2$	38.7	51.7	60.9

[a] Average binding energy determined from the reaction $Au_3(PH_3)_4L_n^{m+} \rightarrow Au_3L_n^{m+} + 4PH_3$.

Table 3. Optimized Au−Au distances (in Å) in the Unit Au_3, with and without Phosphine Ligands and for Singly Ionized Species[a]

system	Au1−Au3	Au1/3−Au2
Au_3	2.52	2.64
$Au_3(PH_3)_4$	2.53	2.79
Au_3^+	2.56	2.56
$Au_3(PH_3)_3^+$	2.60	2.60
$Au_3(PH_3)_4^+$	2.59	2.72

[a] Atoms numbered according to Figure 4.

5.3. Binding Energies. To examine the binding of the different ligand moieties of the Au/In model cluster and their mutual influence, a set of binding energies has been calculated. As these data have been obtained without taking into account geometry relaxation of the various moieties involved, they should only be taken as qualitative measures for comparative purposes. In Figures 5 and 6 the binding energies of the In groups L = $(InCl_2H_2O)$ to the cluster core are given. For both cluster models, with and without phosphine ligands, the μ_2-L group is bound more strongly than the μ_3-L groups. Surprisingly, the bonding of the μ_2- and μ_3-L groups is mutually independent in the sense that the binding energy of μ_2-L is virtually the same if it is attached to Au_3 or to $Au_3(\mu_3\text{-L})_2$ (Figure 5) and *vice versa*. The same observation can be made for the phosphine-ligated models, see Figure 6. In line with this observation, inspection of the one-electron orbitals of $Au_3(PH_3)_4L_3$ shows no mixing between contributions derived from μ_2-In and μ_3-In. Due to phosphine ligation the binding energy of the L groups to the metal cluster core increases, by 16.6 kcal/mol for μ_2-L and by 20.3 kcal/mol for μ_3-L.

This stronger bonding can be attributed to the enhanced donating ability of $Au_3(PH_3)_4$ in comparison to Au_3. On the other hand, it is well-known that phosphine ligation enhances the reactivity of gold since it opens the d shell, facilitating s−d

Table 4. Optimized Bond Lengths (in Å) of the Clusters $Au_3(PH_3)_4(I)_n$, $n = 0-3$[a]

system	Au1−Au3	Au1/3−Au2	Au1−μ_2-I	Au1−μ_3-I	Au2−μ_3-I
$Au_3(PH_3)_4(\mu_2\text{-I})$	2.56	2.75	2.88		
$Au_3(PH_3)_4(\mu_3\text{-I})_2$	2.57	2.90		3.13	2.90
$Au_3(PH_3)_4I_3$[b]	2.57	2.90	2.88	3.04	2.86
exptl[b]					
1	2.56	2.94	2.81	2.85	2.98
2	2.58	2.86	2.79	2.91	2.93

[a] Atoms are numbered according Figure 4. [b] Only the μ_3-I atoms have been relaxed; the Au−Au distances have been taken from $Au_3(PH_3)_4L_2$, and the Au-μ_2-I distance has been taken from $Au_3(PH_3)_4L$. [c] Shown are the corresponding experimental Au−Au and Au−In distances, averaged according to the idealization of C_{2v} symmetry.

hybridization.[12,13,30−31] This effect may be exemplified by the effective configuration of Au2. In Au_3 a configuration of $s^{1.20}$ $p^{0.11}$ $d^{9.80}$ is calculated, which changes to $s^{1.01}$ $p^{0.40}$ $d^{9.57}$ in $Au_3(PH_3)_4$, in good agreement with theoretical findings for other gold compounds containing $AuPH_3$ units.[13,20,32]

Since phosphine ligands play a unique role in gold chemistry,[5a,10a] a detailed discussion of their binding energies is worthwile. In Table 1 the binding energies of the two distinguishable phosphine groups, P1/4H_3 and P2/3H_3, as well as the average phosphine binding energy, calculated from the reaction $Au_3(PH_3)_4L_n \rightarrow Au_3L_n + 4PH_3$, are shown for different cluster subunits. The binding energy for P2/3H_3, which has to share a gold atom with its symmetry partner, is always found to be lower than for the P1/4H_3 groups, which are singly coordinated to a Au center.

Not unexpectedly for a donating ligand, the phosphine binding energy increases with growing oxidation of the gold centers:[13,19] The phosphine−Au bond becomes stronger with increasing number of L groups attached to the Au_3 cluster core (Table 1). (For P2/3H_3 a single exception is found for $Au_3(PH_3)_4$ which may be an artifact due to the unrelaxed geometries employed.) The average phosphine−Au binding energies exhibit this trend, too. They are calculated to be always slightly smaller (by 2−8 kcal/mol) than the averaged binding energies of the individual phosphine groups.

To study the effect of charge on the phosphine binding energy directly, the subclusters $Au_3(PH_3)_4L_n$ ($n = 0-2$) have been ionized in a computer experiment (Table 2). As the average binding energies shown in Table 2 demonstrate, again an increase of the phosphine bond strength with growing cluster charge is found. Interestingly, the trend to larger phosphine binding energies with growing number of L groups, which has been observed for the neutral clusters, is reversed for the 2-fold-ionized species. This effect can be rationalized by observing that the strengthening influence of a positive charge on the Au−P bond decreases with increasing coordination of the Au atoms. While the average phosphine binding energy increases by 41 kcal/mol due to double ionization of $Au_3(PH_3)_4$, the same amount of positive charge results for $Au_3(PH_3)L_2$ in a bond strengthening of only 22 kcal/mol. This counteraction of the effect of positive cluster charging and coordination may prevent the Au/In clusters from further oxidation of the Au atoms without decomposition. Comparison of the phosphine binding energies provides further confirmation of the above assignments of the formal Au oxidation states. The average phosphine binding energy is 42.9 kcal/mol in $Au_3(PH_3)_4L_3$, where the $Au_3(PH_3)_4$ subunit carries a Mulliken charge of +0.77 au; this value compares favorably with the corresponding value of 47.0 kcal/mol for $Au_3(PH_3)_4^+$, where the positive charge models the assumed oxidation state of the Au atoms in the full cluster compound (section 4).

5.4. Geometry Optimization. Since the two very different Au−Au distances found in both Au/In clusters, about 2.6 and 2.9 Å, are the most striking geometric features of these compounds, a series of geometry optimizations on various subunits of a model compound was undertaken. To limit the computational effort, the model cluster was further simplified by replacing the complete In groups (including Cl and H_2O ligands) by iodine centers, resulting in the model cluster $Au_3(PH_3)_4I_3$. This model should apply equally well to both cluster compounds **1** and **2**. The latter cluster newly synthesized in the present work differs from **1** only by the ligands attached to the In centers. Modeling the In groups by iodine centers is motivated by two observations.

As an element of the fifth row, iodine exhibits approximately the same radial extent of the valence orbitals and thus the same atomic size as indium. Furthermore, the number of seven valence electrons corresponds to the formal valence electron count for In in the group ($InCl_2$(thf)) of **1**. The geometry optimization was limited to the distances Au−Au and Au−I, imposing a C_{2v} symmetry constraint. The Au−P bond lengths and orientations and the internal degrees of freedom of the phosphine ligands were kept fixed at the averaged experimental geometry (see above). The optimizations were carried out in a cyclic manner, optimizing each degree of freedom separately until the distances varied were stable to 0.002 Å. To demonstrate systematically the effect of the oxidation state and the different building blocks of the Au/In clusters on the geometry of the central gold triangle, we start the discussion with the bare Au_3 cluster. The moiety Au_3 exhibits a Jahn−Teller distortion $D_{3h} \rightarrow C_{2v}$, as expected from a considerartion of the Au 6s valence orbitals. The bonding orbital a_1 is more strongly localized on Au1/3, and the singly occupied e-type MO (D_{3h} symmetry) splits into the totally symmetric HOMO $2a_1$ and the LUMO b_1. The $2a_1$ MO is bonding between Au1 and Au3, but antibonding with respect to Au2. The difference in bond lengths amounts to 0.11 Å (Table 3), which is considerably smaller than in the Au/In clusters. On the other hand, Au_3^+, which corresponds to the cluster core if the formal oxidation states of the Au atoms are taken literally, forms an equilateral triangle (Table 3).

It is well-known from previous studies on gold clusters[13] that phosphine ligation elongates Au−Au distances, but only to a small amount. This effect is demonstrated here by the C_{3v} symmetric cluster $[Au_3(PH_3)]^+$. Compared to Au_3^+, the Au−Au bond length increases by 0.04 Å (Table 3). A much stronger geometrical effect is observed when four phosphine ligands are added to the Au_3 unit according to their orientation in the Au/In clusters **1** and **2**. For Au_3 the effect of the Jahn−Teller distortion is considerably enhanced, mainly affecting the weaker bonds of Au2. In the case of Au_3^+, the different number of phosphine ligands attached to the gold atoms induces an isosceles shape (Table 3). The Au−Au bond elongation of the

(30) Mingos, D. M. P. *J. Chem. Soc., Dalton Trans.* **1976**, 1164.
(31) De Kock, R. L.; Baerends, E. J.; Boerrigter, P. M.; Hengelmolen, R. *J. Am. Chem. Soc.* **1984**, *106*, 3387.
(32) Pyykkö, P.; Angermaier, K.; Assmann, B.; Schmidbaur, H. *J. Chem. Soc., Chem. Commun.* **1995**, 1889.

2-fold-ligated Au atom can be rationalized by the fact that the electron donation of phosphine ligands pushes the highest occupied orbital of the gold atoms to higher energy.[30] In our study, the HOMO of $Au(PH_3)_2$ is found to lie 22 kcal/mol higher in energy than the HOMO of $Au(PH_3)$. Consequently, the bonding a_1 MO of Au_3^+ becomes more localized on Au1/3 and the Au−Au bonds to Au2 increase. The same argument applies in the case of neutral $Au_3(PH_3)_4$.

The difference between the two intergold distances amounts to 0.26 Å in $Au_3(PH_3)_4$ and 0.13 Å in $Au_3(PH_3)_4^+$. The latter difference in the Au−Au distances is considerably smaller than in the parent cluster compounds (**1**, 0.37 Å; **2**, 0.29 Å). Thus, besides the oxidation of one Au atom, an additional effect of the In groups is to be expected. The results of geometry optimizations including iodine atoms as models of the In groups are given in Table 4. The moiety μ_2-I, which acts mainly on the stronger bond Au1−Au3, has only a minor influence on the intergold bond lengths. Compared to $Au_3(PH_3)_4$ the shorter bond is elongated by 0.03 Å while the longer one shrinks by 0.04 Å. As could have been expected, due to the addition of a single electron-withdrawing group, a geometry of the gold triangle intermediate between $Au_3(PH_3)_4$ and $Au_3(PH_3)_4^+$ is adopted (cf. Table 3). A considerably stronger change in geometry is observed when two μ_3-I atoms are added. This interaction affects predominantly the weak Au1/3−Au2 bond, which increases by 0.11 Å. We refrained from an optimization of all 5 degrees of freedom of the complete model $Au_3(PH_3)_4I_3$. Since the effect of μ_2-I on the intergold distances has been shown to be moderate, we fixed the intergold distances according to the model $Au_3(PH_3)_4(\mu_3\text{-I})_2$ and reoptimized only the position of the μ_3-I atoms. Overall, a fairly good estimate of the geometry of the central Au_3 units of the Au/In clusters was achieved: The difference of the intergold distances is calculated to be 0.33 Å, which compares favorably with the experimental results, 0.37 Å for **1** and 0.29 Å for **2**. The absolute values of both distances lie between the values found experimentally for the compounds **1** and **2** (Table 4).

On the basis of results of these model calculations we may also rationalize the differences of the Au−Au distances in the two Au/In clusters **1** and **2**. The Au1−Au3 bond in **2** is slightly longer and the bonds to Au2 are shorter than in **1** (Table 4). Qualitatively the same trend is observed as a result of ionizing $Au_3(PH_3)_4$. Thus, a more positive charge is suggested for the central $Au_3(PH_3)_4$ unit in **2** as compared to its Cl-ligated analogue. A closer look at the differences between the two clusters reveals that this suggestion is quite plausible. Besides the substitution of Cl by Br in **2**, two thf groups are replaced by a bridging Br. The electron-withdrawing power of the additional Br atom is balanced by an extra electron, yielding an anionic Au/In cluster. Although Br is slightly less electronegative than Cl, a lower electronic charge has to be attributed to the Au_3 unit in **2** than in **1**, since the electron count of two In atoms is lowered by 2 due to the substitution of the donating thf groups by a Br^- anion. Thus, the electron-withdrawing capability of the corresponding In groups should be enhanced, leading to a more positive charge of the $Au_3(PH_3)_4$ unit, in agreement with the trend derived from the comparison with our model calculations.

Given the simplicity of our model cluster, it does not come as a surprise that the calculated Au−I distances do not resemble the measured Au−In bond lengths too closely (Table 4). Although a reoptimization of μ_3-I in $Au_3(PH_3)_4I_3$ showed a considerable relaxation of the bonds involved, no closer agreement with experiment was achieved. Thus, while the model chosen has been demonstrated to be successful for simulating and rationalizing the geometry of the central Au_3 unit, a quantitative comparison of metal−ligand bond lengths Au−I and Au−In is beyond its scope.

5.5. Summary. Scalar relativistic all-electron density functional calculations on model compounds of the Au/In clusters have been performed, aiming at a clarification of the oxidation states of the Au and In atoms as well as at a rationalization of the observed considerable differences in the Au−Au bond lengths.

The two different oxidation states previously assigned to the Au atoms were found plausible as judged by a Mulliken population analysis. For the In atoms, on the other hand, no interpretable differences of Mulliken charges were obtained and we resorted to assigning the same intermediate oxidation state to both of them.

We were able to trace the origin of the two very different Au−Au bond lengths in the Au/In clusters by means of a series of geometry optimizations of subunits of the model compound $Au_3(PH_3)_4I_3$. Two effects are involved: A charge imbalance is induced on the central Au triangle due to the 2-fold phosphine ligation of one of the Au atoms. The resulting weaker bond of the 2-fold-ligated metal atom is further reduced in strength by the electron-withdrawing μ_3-In groups, leading to a final difference of about 0.3 Å between the two Au−Au distances. Furthermore, the deviations in the Au−Au bond lengths between the Cl- and Br-ligated Au/In cluster species were rationalized by a more positive charge of the $Au_3(PH_3)_4$ unit in agreement with a corresponding trend for these bond lengths calculated for the isolated neutral and singly ionized moiety $Au_3(PH_3)_4$.

Acknowledgment. This work was supported by Deutsche Forschungsgemeinschaft and Fonds der Chemischen Industrie. F.P.G. thanks the Alexander von Humboldt Foundation for a research fellowship. S.-C.C. is grateful to the Deutscher Akademischer Austauschdienst for a graduate student scholarship. Support by Degussa AG and Heraeus GmbH through the donation of chemicals is acknowledged. Mr. J. Riede is thanked for collecting the X-ray data sets and Katrin Albert for assistance in the preparation of some of the figures.

Supporting Information Available: Tables listing detailed crystallographic data, atomic positional parameters, and bond lengths and angles (17 pages). Ordering information is given on any current masthead page.

IC970725C